Continuum in the Spin-Excitation Spectrum of a Haldane Chain Observed by Neutron Scattering in $CsNiCl_3$

I. A. Zaliznyak,[1] S.-H. Lee,[2,3] and S. V. Petrov[4]

[1]*Department of Physics, Brookhaven National Laboratory, Upton, New York 11973-5000*
[2]*National Institute of Standards and Technology, Gaithersburg, Maryland 20899*
[3]*Department of Physics, University of Maryland, College Park, Maryland 20742*
[4]*P. Kapitza Institute for Physical Problems, ulica Kosygina, 2, Moscow, 117334 Russia*

(Received 4 October 2000; published 15 June 2001)

The spin-excitation continuum, expected to dominate the low-energy fluctuation spectrum in the Haldane spin chain around the Brillouin zone center, $q = 0$, is directly observed by inelastic magnetic neutron scattering in the $S = 1$ quasi-1D antiferromagnet $CsNiCl_3$. We find that the single mode approximation fails, and that a finite energy width appears in the dynamic correlation function $S(q, \omega)$ for $q \lesssim 0.5\pi$. The width increases with decreasing q, while $S(q, \omega)$ acquires an asymmetric shape qualitatively similar to that predicted for the two-magnon continuum in the nonlinear σ-model.

DOI: 10.1103/PhysRevLett.87.017202 PACS numbers: 75.10.Jm, 75.40.Gb, 75.50.Ee

A remarkable prediction by Haldane [1], that a one-dimensional (1D) Heisenberg antiferromagnet (HAFM) with integer spin has a gap in the spin excitation spectrum and a finite correlation length even at $T = 0$, put 1D $S = 1$ HAFM in the focus of a continued research activity. By now, experiments [2–5] and numerical studies [6–11] provided a spectacular confirmation of the Haldane conjecture. It was established that the correlation length is $\xi \approx 6$ lattice repeats, and the Haldane gap is $\Delta_H \approx 0.41J$ (J is the exchange coupling). The excitations' spectral weight is concentrated in a long-lived massive triplet mode in the vicinity of the Brillouin zone (BZ) boundary $q = \pi$. The nonlinear σ model (NLσM), which gives a valid description of the 1D $S = 1$ HAFM in the long-wavelength limit [11–13], and the variational treatment based on the Jordan-Wigner fermionization of the spin operators [14], predict that the lowest-energy excitations near $q = 0$ are pairs of $q \approx \pi$ magnons. In the absence of magnon interaction, the two-magnon continuum at $q = 0$ starts above a gap of $2\Delta_H$. Monte Carlo (MC) numerical experiments and the exact diagonalization (ED) for rings of up to 18 spins not only support this claim [6–9], but also suggest that continuum exists at $|q| \lesssim 0.5\pi$, almost in the half of a Brillouin zone.

In spite of a solid theoretical evidence for existence of the $q \approx 0$ continuum in the spectrum of a 1D $S = 1$ HAFM, its limits and extent remain unclear and controversial. In fact, in neutron scattering studies of magnon dispersion in the model Haldane compound NENP [3], no appreciable deviation from the single mode approximation (SMA) was found for $q \geq 0.3\pi$. Consequently, a picture for the excitation spectrum of the 1D $S = 1$ HAFM, where a single-magnon dispersion merges into a broad, but unmeasurable, continuum at $q < 0.3\pi$, became broadly popular [6,10]. In this paper we report a high resolution neutron scattering study of the quasi-1D $S = 1$ HAFM $CsNiCl_3$ which corrects this picture and presents the first resolved measurement of the continuum part of the excitation spectrum of a Haldane spin chain.

To describe a single-magnon part of the 1D excitation spectrum in $CsNiCl_3$ we use a lattice periodic dispersion,

$$\varepsilon(q) = \sqrt{\Delta_H^2 + v^2 \sin^2 q + \alpha^2 \cos^2 \tfrac{q}{2}}\,, \qquad (1)$$

obtained in the physically motivated semiquantitative theory [14] (solid lines in Figs. 1 and 3). This simple theory correctly captures the fermionlike nature of the $q \approx \pi$ magnons found in experiment [15], and provides an

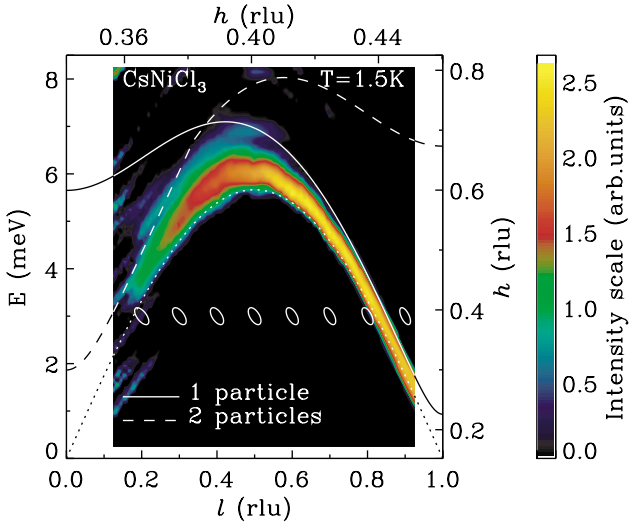

FIG. 1 (color). Contour plot of the measured spectral density of magnetic scattering, reconstructed from nine constant-q scans via linear interpolation. Scale on the right shows variation with energy of the wave vector transfer perpendicular to the chain at $l = 0.5$, scale on the top—its variation with l at $E = 3$ meV. Ellipses are the half maximum contours of the instrument resolution function, calculated at $E = 3$ meV. Solid curve is the single-magnon dispersion (1), dashed line shows the lowest energy of the two noninteracting magnons with given total $q = \pi l$, and dotted line is $\varepsilon(q) = v \sin q$.

 © 2001 The American Physical Society

appealing analytical description of the excitation spectrum in a Haldane chain, with the single-magnon dispersion crossing the two-particle energy at $q \lesssim \pi/2$. At $q \gtrsim \pi/2$ Eq. (1) is in very good agreement with MC [6]. It was also found to coincide with the dispersion, measured in NENP at $q \gtrsim 0.3\pi$, if the parameter α is adjusted from $\alpha \approx 2.5J$ [14] to $\alpha \approx 1.45J$ [3]. Using $J = 2.275$ meV, independently determined from the high field magnetization [16], we find that Eq. (1) gives an excellent fit to the excitation energies in $CsNiCl_3$. We obtain $v = 2.49(4)J$ and $\alpha \approx 1.1J$, in remarkable agreement with the numerical result [11]. Most importantly, we find that spectral density deviates from the SMA at $q \lesssim 0.5\pi$, where a crossover to the excitation continuum occurs.

The experimental characterization of the continuum is hindered by the rapid decrease of the static spin structure factor $S(q) = \int S(q,\omega)\, d(\hbar\omega)$ at small q. It follows from the first moment sum rule [17], which establishes an *exact* relation between $S(q)$ and the excitation average energy $\langle\varepsilon(q)\rangle = \int(\hbar\omega)S(q,\omega)\, d(\hbar\omega)/\int S(q,\omega)\, d(\hbar\omega)$. For the 1D $S = 1$ HAFM,

$$S(q) = -\frac{2}{3} E_{\mathrm{GS}} \frac{(1 - \cos q)}{\langle\varepsilon(q)\rangle}, \qquad (2)$$

where $E_{\mathrm{GS}} = -1.40(0)J$ [10] is the ground state (GS) energy per site. For a gapful spectrum $S(q)$ of Eq. (2) vanishes $\sim q^2$ at $q \to 0$. Where SMA holds, $S(q)$ is uniquely determined by the dispersion, $\langle\varepsilon(q)\rangle \equiv \varepsilon(q)$. Observation of the continuum is also hindered if the excitation spectrum is split by the anisotropy, as in NENP and related Ni-organic model compounds, or if the excitations acquire a temperature-activated damping.

$CsNiCl_3$ is one of the most isotropic and best studied quasi-1D $S = 1$ HAFM compounds (see [4,5], and references therein). It has a hexagonal crystal structure, space group $P63/mmc$; at $T = 1.5$ K the lattice spacings are $a = 7.12$ Å and $c = 5.9$ Å. Chains of Ni^{2+} ions run along the c axis and form a triangular lattice in the a-b plane. There are two equivalent ions per c spacing, so that $\boldsymbol{Q} = (h,k,l)$ in reciprocal lattice units corresponds to $q = \pi l$ in the 1D BZ of a chain. A very reliable estimate for the in-chain exchange coupling, $J = 2.275$ meV, is obtained from the measured spin-flip (saturation) field $H_s = 4Jg\mu_B S = 73.5$ T [16]. A spin-flop (reorientation) field $H_{\mathrm{sf}} \approx 1.9$ T implies a negligible single-ion anisotropy, $D \approx 0.002J$.

The main disadvantage of $CsNiCl_3$ as a model 1D HAFM is the supercritical interchain coupling $J_\perp$, which leads to a 3D order with the propagation vector $\boldsymbol{Q}_0 = (1/3, 1/3, 1)$, at $T_N \approx 4.8$ K. The relevance of the Haldane conjecture in this situation was the subject of a long-lasting controversy. It was established that a gap opens in the spin-excitation spectrum at $T > T_N$, and in this so-called "1D phase" it recovers the features of a Haldane chain. However, since $T_N \approx 0.2J$, the spectrum also acquires significant temperature broadening [5] which hinders the identification of a continuum. On the other hand, the spectrum also regains the 1D character at high energies, where excitations, whose energy is sufficiently large compared to $J_\perp$, are not sensitive to it. Later on we will present quantitative arguments which show that weak 3D order in $CsNiCl_3$ causes no significant change in the spectrum throughout the better part of the BZ. And indeed, experiments show that the Haldane gap triplet mode is split in the 3D ordered phase only in the close vicinity of the magnetic Bragg peaks, at $|q| \gtrsim 0.9\pi$, where the Goldstone acoustic magnons appear [4,5]. Also, the elastic Bragg intensity, corresponding to the ordered spin value $\langle S\rangle = 0.5$, observed in experiment [18], accounts for only $\langle S\rangle^2/[S(S+1)] = 12.5\%$ of the spin fluctuation spectrum. In the 1D $S = 1$ HAFM this fraction of the spectral weight is concentrated in the tiny region of the BZ, at $0.98\pi \lesssim |q| \leq \pi$.

We measured the dependence of the energy spectrum of the spin dynamic structure factor on the wave vector transfer along the chains for a $CsNiCl_3$ sample made of two large crystals with total mass 6.4(1) g, at $T = 1.5$ K. The sample was mounted with the (h,h,l) zone in the scattering plane, and had effective mosaic spread $\lesssim 1°$. Measurements were done on SPINS 3-axis cold neutron spectrometer at NIST Center for Neutron Research. It is equipped with an $\approx$22 cm wide PG(002) analyzer, which allows one to increase the data collection rate by opening the wave vector acceptance. We used a position sensitive detector (PSD) matched in size to the (flat) analyzer whose central energy was fixed at $E_f^{(0)} = 4.2$ meV and angular acceptance was $\approx 9°$. In this setup both the energy E_f and the wave vector $\mathbf{k}_f$ of neutrons reflected at different points across the analyzer vary, but the $\mathbf{k}_f$ component along the analyzer scattering vector $\boldsymbol{\tau}_A$ is constant [19]. Calibration of the neutron final energy and the sensitivity across the PSD was done using elastic incoherent scattering from vanadium. Beam divergence was defined by the ^{58}Ni neutron guide and a $80'$ radial collimator in front of the PSD. To perform energy scans at constant $q = \pi l$, chains were always aligned parallel to $\boldsymbol{\tau}_A$. Typical variation of the wave vector transfer along [110] imposed by this condition is illustrated by the right and top axes of Fig. 1. It shows the contour plot of the raw spectral density of the scattering intensity $[\sim I(q,E)/\int I(q,E)\, dE]$, with the q-dependent flat background subtracted. It is evident from Fig. 1 that the spectrum acquires a finite width in energy at $l \lesssim 0.5$. Although the effect is somewhat exaggerated by the resolution, careful accounting for the latter shows that *intrinsic* width, where it is nonzero, accounts for $\sim 2/3$ of the total width. Curves show the prediction of [14], obtained from (1) with $J = 2.275$ meV, $\Delta_H = 0.41J$, $v = 2.49J$, and $\alpha = v$.

For the quantitative analysis of the energy dependence of the measured cross section, we use the normalized scattering function of the damped harmonic oscillator (DHO), parametrized in terms of the position ω_0, and the full width at half maximum (FWHM) of the corresponding antisymmetrized Lorentzian peak [5]. To describe the asymmetric peak at lower q we use a "half-Lorentzian" truncated DHO (TDHO), which gives a good analytical approximation of

the two-magnon line shape, predicted by the NLσM [12]. It is obtained by multiplying the $S(q, \omega)$ of the DHO with a step function $\theta(\omega^2 - \omega_0^2)$. At $q > \pi/2$, where the SMA holds, both DHO and TDHO line shapes become δ functions. Our resolution correction [20] procedure is identical with that used in Ref. [3]. The resolution-convoluted TDHO fits to several constant-q scans are shown in Fig. 2. As quantified by χ^2 in Fig. 3(d), TDHO is in better agreement with experiment at $q \lesssim 0.5\pi$, where a sharper onset of the scattering at low energies, characteristic of a continuum, is observed. Note that an *opposite* asymmetry, which is a purely resolution effect, was reported in Ref. [3].

Peak parameters, refined for both DHO and TDHO fits, are detailed in Fig. 3. The dispersion of the center of mass of the excitation spectrum, captured by the position of the DHO peak [circles in Fig. 1(a)], is nicely described by Eq. (1). For $J = 2.275$ meV, the best fit, shown in the figure, gives $\Delta_H = 0.34(6)J$, $v = 2.49(4)J$, and $\alpha = 1.1(4)$. While at $q \leq 0.9\pi$ the spectrum is not very sensitive to Δ_H; the agreement of the magnon velocity v with calculations [11] is impressive. The energy integrated intensity of both DHO and TDHO peaks, Fig. 3(b), is in good agreement with the sum rule (2).

The peaks at $q \lesssim 0.5\pi$ are very similar in shape and intensity to the two-magnon continuum in the 1D NLσM [12], which we show by the dotted lines in Fig. 2. Even though we used the realistic magnon dispersion (1), instead of the relativistic form $\varepsilon(q) = \sqrt{\Delta_H^2 + (v\tilde{q})^2}$, $\tilde{q} = q \bmod \pi$, which fails for $\tilde{q} \gtrsim 0.2\pi$, the calculated continuum is still too high in energy. In fact, this discrepancy does not simply show the limitation of the σ model, but

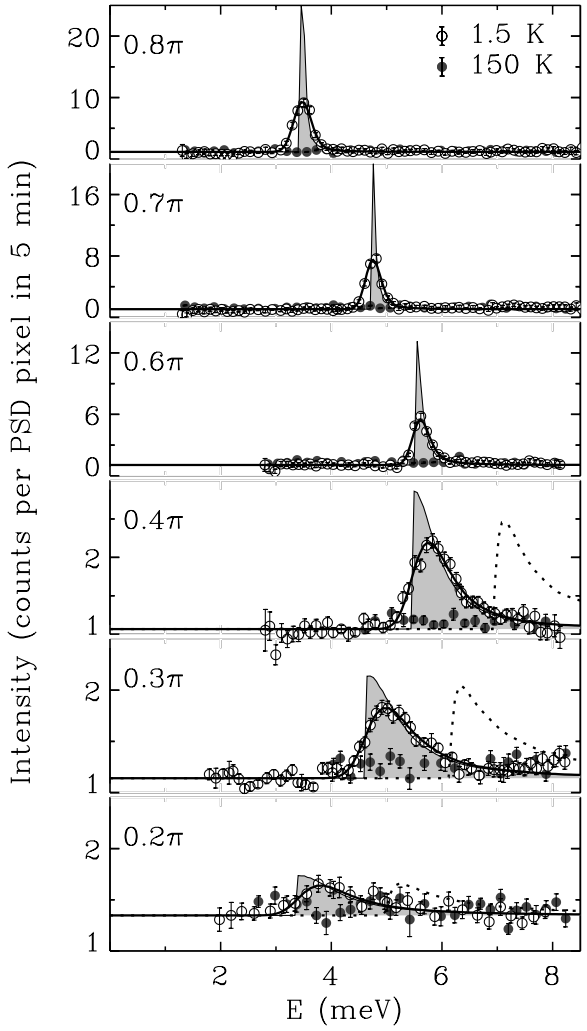

FIG. 2. Energy spectrum of the inelastic scattering, measured in $CsNiCl_3$ at several $q = \boldsymbol{Q}\boldsymbol{c}/2 = \pi l$. The wave vector component in the a-b plane $q_\perp = \boldsymbol{Q}\boldsymbol{a} + \boldsymbol{Q}\boldsymbol{b} = \pi h\sqrt{3}$ is defined by the scattering geometry $\boldsymbol{c} \parallel \tau_A$ (Fig. 1). Solid circles show the nonmagnetic background. Thick lines are the resolution-corrected fits to the TDHO cross section. Shaded peaks are the same cross section, normalized by the resolution volume, and illustrate the "deconvoluted" intensity. Dotted lines show the two-magnon continuum in the NLσ model [12], corrected for the nonrelativistic dispersion (1).

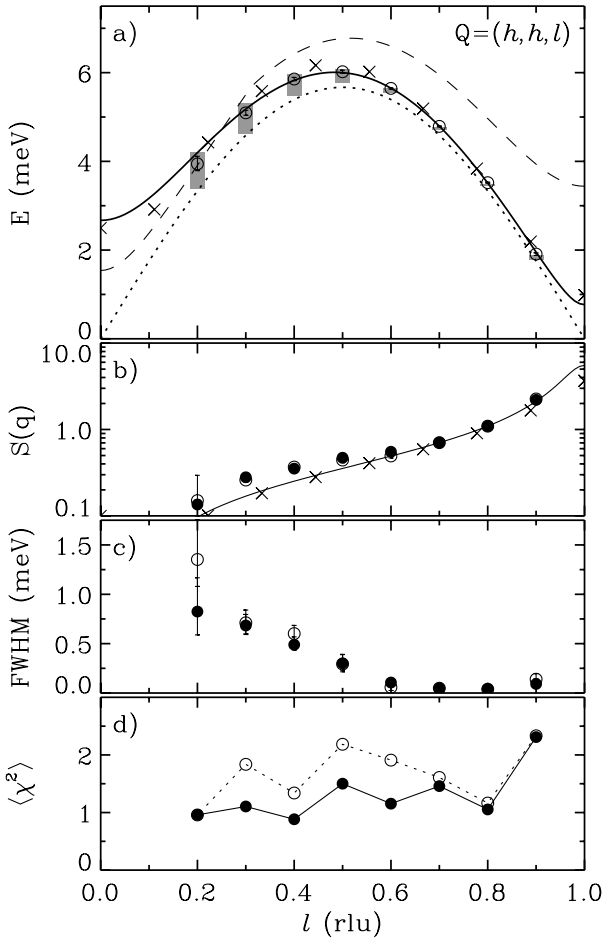

FIG. 3. Wave vector dependence of the excitation spectrum in $CsNiCl_3$. Full and open circles show the parameters obtained for the asymmetric TDHO and symmetic DHO line shapes, respectively. Crosses are ED results [6]. (a) Shaded bars start at the lower boundary of the asymmetric TDHO peak, and extend by its FWHM. Circles show the Lorentzian peak position of the symmetric DHO fits. Lines are the same as in Fig. 1, but with $\Delta_H = 0.34J, \alpha = 1.1J$. (b) Static structure factor. Line is the SMA result for the dispersion shown in (a). (c) Peak intrinsic FWHM. (d) Chi square for the TDHO and DHO fits.

also reveals the importance of magnon interactions. Indeed, a careful examination of Figs. 1 and 3(a) shows that the lower boundary of the observed continuum lies *below* the lowest energy of two noninteracting magnons. This could be understood, if there is an *attraction* between the quasiparticles, which form the continuum states.

To understand how our findings compare with existing results, it is important to realize that the extent of the observed continuum is rather small, as is predicted by the NLσM. At $q = 0.3\pi$, the FWHM is $\approx 0.3J$, or only $\approx 15\%$ of the peak energy, and requires high resolution and low temperature, $T \ll 0.3J$, to be detected. Previous attempts to measure the in-chain dispersion in $CsNiCl_3$ [4] were, on the contrary, done with rather coarse resolution of the thermal neutron spectrometer, and at $T \sim 0.4J$, where temperature damping dominates the spectral width. It is more interesting to compare our results with the neutron scattering study in NENP [3], where no appreciable deviation from the SMA was found at $T \lesssim 0.01J$ for $q \geq 0.3\pi$. This result, however, is easily reconciled with our data, if we note that, to observe magnetic scattering at small q, the authors had to relax the spectrometer resolution so much that almost a quarter of the 1D dispersion was within their wave vector acceptance. The effect we observe is simply unresolved in such a measurement. The splitting of the spectrum by single-ion anisotropy, which is rather large in NENP [15], presented another obstacle to the characterization of the continuum there.

Finally, before drawing conclusions, we evaluate *quantitatively* the effect of the interchain coupling and 3D order on the excitation spectrum of the quasi-1D $S = 1$ HAFM in the mean field (MF) random phase approximation (RPA), and show that it is not important in our case. The excitation integral intensity, given by the right-hand side of Eq. (1), is modified in three ways. (i) The Heisenberg exchange energy changes on account of the static order. At $\langle S \rangle \lesssim 0.5$ the staggered magnetization of a Haldane chain is still linear [21], and in the MF approximation the energy change is $\langle S \rangle^2/(2\chi_\pi)$, or less than 0.5%, due to the large static staggered susceptibility $\chi_\pi \approx 22/J$ [9]. (ii) The numerator has to be amended by adding the interchain correlation, $\sum_{\beta,\boldsymbol{\tau}_\perp} J_\perp[1 - \cos(\boldsymbol{q}_\perp \cdot \boldsymbol{\tau}_\perp)] \times \langle S^\beta_{\mathbf{R}} S^\beta_{\mathbf{R}+\boldsymbol{\tau}_\perp} \rangle$, where $\boldsymbol{q}_\perp$ is the wave vector component, perpendicular to the chain. In MF this is $\approx \frac{1}{2}[J_\perp(0) - J_\perp(\boldsymbol{q}_\perp)]\langle S \rangle^2 \leq \frac{9}{2} J_\perp \langle S \rangle^2$, where $J_\perp(\boldsymbol{q}_\perp)$ is the Fourier transform of the interchain coupling, and can be neglected if $\frac{9}{2} J_\perp \langle S \rangle^2 \ll -\frac{2}{3} E_{\mathrm{GS}}(1 - \cos q)$. (iii) The interchain dispersion, introduced by $J_\perp$, changes the magnon energy and the denominator of Eq. (1). In RPA this is given by $\varepsilon(q, \boldsymbol{q}_\perp) \approx \varepsilon(q)\sqrt{1 + \chi_q J_\perp(\boldsymbol{q}_\perp)} \approx \varepsilon(q) + S(q) J_\perp(\boldsymbol{q}_\perp)$. Here $\varepsilon(q)$ and $\chi_q = 2S(q)/\varepsilon(q)$ are the magnon energy and the spin susceptibility of a single chain, respectively. From the boundaries of the interchain dispersion at $q = \pi$, measured for $CsNiCl_3$ in [4] at $T \approx 10$ K, and using $\chi_{\pi, T \approx 0.4J} \approx 0.74 \chi_{\pi, T=0}$ [3], we find $\max\{J_\perp(\boldsymbol{q}_\perp)\} - \min\{J_\perp(\boldsymbol{q}_\perp)\} = 9J_\perp \approx 0.3J$. Plugging this value in the above estimates, we conclude that the purely 1D expressions for the magnon dispersion and the energy integrated scattering intensity hold for $CsNiCl_3$ within $\pm 5\%$ at $0.3\pi \lesssim q \lesssim 0.7\pi$, and within $\pm 10\%$ at $0.2\pi \lesssim q \lesssim 0.8\pi$.

Thus, our measurements present a detailed characterization of the nonhydrodynamic part of the excitation spectrum in the 1D $S = 1$ HAFM. We find that single mode dispersion gradually crosses over to a *narrow continuum* at $q \lesssim 0.5\pi$. The continuum starts *below* the lowest possible energy of the two noninteracting magnons, indicating their *attraction*.

We gratefully acknowledge discussions with C. Broholm, L.-P. Regnault, and A. Zheludev, which inspired us throughout this study. This work was carried out under Contract No. DE-AC02-98CH10886, Division of Materials Sciences, U.S. Department of Energy. The work on SPINS was supported by NSF through DMR-9986442.

[1] F. D. M. Haldane, Phys. Lett. **93A**, 464 (1993); Phys. Rev. Lett. **50**, 1153 (1983).
[2] J.-P. Renard *et al.,* Europhys. Lett. **3**, 949 (1987); L.-P. Regnault *et al.,* Phys. Rev. B **50**, 9174 (1994).
[3] S. Ma *et al.,* Phys. Rev. Lett. **69**, 3571 (1992); Phys. Rev. B **51**, 3289 (1995).
[4] W. J. L. Buyers *et al.,* Phys. Rev. Lett. **56**, 371 (1986); R. M. Morra *et al.,* Phys. Rev. B **38**, 543 (1988); Z. Tun *et al.,* Phys. Rev. B **42**, 4677 (1990).
[5] M. Steiner *et al.,* J. Appl. Phys. **61**, 3953 (1987); I. A. Zaliznyak *et al.,* Phys. Rev. B **50**, 15 824 (1994).
[6] M. Takahashi, Phys. Rev. Lett. **62**, 2313 (1989); Phys. Rev. B **48**, 311 (1993); **50**, 3045 (1994).
[7] S. V. Meshkov, Phys. Rev. B **48**, 6167 (1993); J. Deisz, M. Jarrell, and D. L. Cox, Phys. Rev. B **48**, 10 227 (1993).
[8] S. Yamamoto, Phys. Rev. Lett. **75**, 3348 (1995).
[9] O. Golinelli *et al.,* Phys. Rev. B **46**, 10 854 (1992); J. Phys. Condens. Matter **5**, 1399 (1993); S. Haas *et al.,* Phys. Rev. B **48**, 3281 (1993).
[10] S. R. White, Phys. Rev. Lett. **69**, 2863 (1992); S. R. White and D. A. Huse, Phys. Rev. B **48**, 3844 (1993).
[11] E. S. Sorensen and I. Affleck, Phys. Rev. B **49**, 13 235 (1994); **49**, 15 771 (1994).
[12] I. Affleck and R. A. Weston, Phys. Rev. B **45**, 4667 (1992).
[13] P. Horton and I. Affleck, cond-mat/9907431.
[14] G. Gómez-Santos, Phys. Rev. Lett. **63**, 790 (1989).
[15] L.-P. Regnault *et al.,* J. Phys. Condens. Matter **5**, L677 (1993).
[16] H. A. Katori *et al.,* J. Phys. Soc. Jpn. **64**, 3038 (1995).
[17] P. C. Hohenberg and W. F. Brinkman, Phys. Rev. B **10**, 128 (1974).
[18] W. B. Yelon and D. Cox, Phys. Rev. B **7**, 2024 (1972).
[19] I. Zaliznyak *et al.* (to be published).
[20] N. D. Chesser and J. D. Axe, Acta Crystallogr. Sect. A **29**, 160 (1973).
[21] A. Zheludev *et al.,* Phys. Rev. Lett. **80**, 3630 (1998).